ЯДЕРНА ФІЗИКА ТА ЕНЕРГЕТИКА 2010, т. 11, № 4, с. 394 - 399

УДК 539.172

DISSIPATIVE PROCESSES IN $^{18}O + ^{9}Be$ AND $^{18}O + ^{181}Ta$ REACTIONS AT FERMI ENERGIES

© 2010 B. Erdemchimeg[1,2], T. I. Mikhailova[1], A. G. Artyukh[1], G. Kaminski[1,3], Yu. M. Sereda[1,4], M. Colonna[5], M. Di Toro[5], H. H. Wolter[6]

[1] *Joint Institute for Nuclear Research, Dubna, Moscow region, Russia*
[2] *Mongolian National University, NRC, Ulaanbaatar, Mongolia*
[3] *Institute of Nuclear Physics, Polish Academy of Sciences, Krakow, Poland*
[4] *Institute for Nuclear Research, National Academy of Sciences of Ukraine, Kyiv*
[5] *Laboratorio Nazionale del Sud, Istituto Nazionale di Fisica Nucleare, Catania, Italy*
[6] *Faculty of Physics, University of Munich, Garching, Germany*

A study of peripheral nuclear collisions at Fermi energies with transport models is presented. It is motivated by experiments devoted to studying of isotopic yields in the reactions ^{18}O on ^{9}Be and ^{181}Ta at E/A = 35 MeV measured at very forward angles. The data show a two-component structure, one centered at beam velocity ("direct component") and another at lower velocities ("dissipative component"). It is shown that the transport calculations describe the general features of the dissipative component of the reaction. In our calculations we take into account the evaporation of the excited, primary projectile-like residues due to statistical decay. This improves the comparison of the results of the calculations with experiment. We find substantially different behavior of the dissipative component in the reactions with light and heavy target.

Keywords: deep inelastic reactions, transport models, Fermi energy.

Introduction

Heavy ion collisions at Fermi energies ($E/A \sim 37$ MeV) are a source of production of new isotopes [1]. The mechanism of these processes, however, is still debated. With increasing energy it should evolve from dissipative to direct breakup and finally to multifragmentation processes. In the Fermi energy region it is expected that the first two processes can coexist and in this paper we study this situation theoretically. In the experiment isotope yields and velocity distributions have been investigated. The latter often show an asymmetric behavior with a maximum close to beam velocity and a low energy tail or shoulder. This suggests the contributions of the above two reaction mechanisms. Various approaches have been made to describe these asymmetric distributions theoretically in an empirical way [2, 3], either by separating the two components [4 - 6], or by using asymmetric distributions [7, 8].

In this contribution, we present a theoretical analysis [9] of velocity and isotope distributions of projectile-like fragments in the reaction ^{18}O on ^{181}Ta and ^{9}Be targets at E/A = 35 MeV measured at the FLNR laboratory in Dubna [10, 11]. In this experiment fragments were detected in the narrow range of forward angles $|\Delta\theta| \leq 2.5$ deg. In our analysis we use the approach to decompose these velocity distributions into two components: one component centered at beam velocity (called direct or breakup, BU) and a dissipative or deep-inelastic component (DIC) that peaks at velocities below the beam velocity [9]. We use semi-classical transport theory to theoretically describe the heavy ion reaction, and we find that in this framework only the dissipative component can be described [9, 12, 13]. The direct component can be interpreted in the Goldhaber model [14]. In this contribution we will discuss the theoretical aspects of the dissipation in the two reactions, particularly, the comparison of the reactions on light and heavy targets. The comparison with the experiment has been shown in [13].

The fragments produced in the transport calculation at the freeze-out configuration are still considerably excited, and will evaporate further particles before they are detected. This secondary evaporation has to be taken into account when comparing to experimental data. In this contribution we investigate, in particular, the effect of this secondary evaporation on the velocity spectra and isotope distributions. We use the Statistical Multifragmentation Model (SMM) of Bondorf, Mishustin and Botvina [15]. A critical ingredient in this model is a good estimate of the excitation energy of the primary fragments that emerge from the transport calculations.

Transport and statistical decay calculations

The transport calculations are performed in the Boltzmann-Nordheim-Vlasov (BNV) approach, which describes the time evolution of the one-body phase space distribution function $f(r, p, t)$ under the influence of a Vlasov mean field $U(f)$ and a Boltzmann two-body collision term I_{coll}, which includes the effect of Pauli blocking [16]. It is solved by simulations using the test-particle method. For more details we refer to [17].

The evolution of the reaction is followed until the freeze-out time, determined by the condition that the fragments are interacting essentially only by Coulomb forces [9, 12]. The primary fragments, in this case the projectile- and target-like residues, produced at freeze-out are still excited with energies of the order of a few MeV per nucleon. In order to realistically compare the results of the calculation with experimental data, we include the de-excitation of the primary fragments by nucleon and light particle evaporation using the Statistical Multifragmentation Model. This model, given the mass, charge and excitation energy of a fragment, will calculate the isotope distributions, coordinates and velocities of the final, cold products. After matching with Coulomb trajectories we also obtain the final velocity distributions of fragments. The crucial quantity is the value of excitation energy. In this contribution we explore the influence of the de-excitation using the following estimate for the excitation energy. The total excitation energy is given as

$$E_{exc} = (E_{\text{kin}} + E_{\text{pot}})_{t=0} - (E_{\text{kin}} + E_{\text{pot}})_{\text{t=freeze-out}} - E_{\text{kin}}^{\text{lost.part}},$$

where the potential energy of a fragment is calculated from the Bethe - Weizsäcker mass formula. The term at freeze-out includes only the projectile- and target-like residues. The term $E_{\text{kin}}^{\text{lost.part}}$ takes into account the energy carried away by the early emitted pre-equilibrium particles. We use a constant value of 15 MeV per nucleon, corresponding approximately to the mean kinetic energy of the evaporated nucleons. The excitation energy is distributed between the two main fragments proportionally to their mass, corresponding to an equal temperature, which might be appropriate at these energies. In Fig. 1, *a* the calculated average excitation energies per nucleon are shown for binary reactions as a function of the impact parameter normalized to $(R_1 + R_2)$. It is seen that the excitation energies are somewhat higher in the reaction with Be (note that the kinetic energy available in the center of mass system is larger for lighter target), and they rise to about 2 or 3 MeV per nucleon for the smallest impact parameters which still lead to binary processes. We emphasize that the above estimate of the excitation energy serves as a first guideline. Excitation energies will be calculated in the future more consistently with the same mean field approach as in the transport calculation.

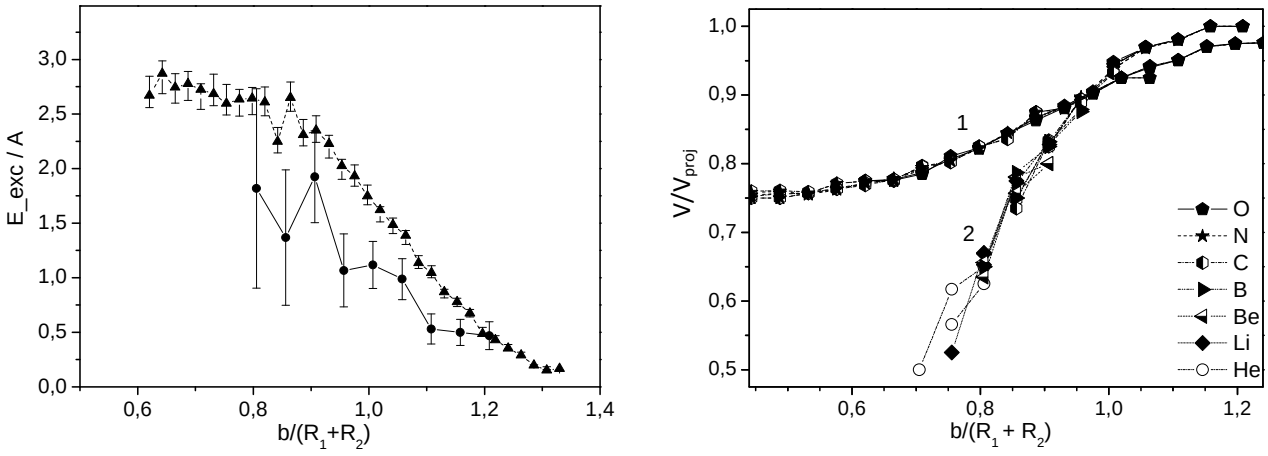

a *b*

Fig. 1. *a* – Excitation energy per nucleon as a function of impact parameter (normalized to the sum of the radii) for the reaction O on Be (triangles) and Ta (circles) at E/A = 35 MeV. *b* – Velocities (ratio to beam velocity) of the projectile-like fragments (maxima of the velocity distribution) as a function of the normalized impact parameter for the reactions on Be (labeled "1") and on Ta ("2"). Different elements are distinguished by different symbols.

Results

We start to discuss some general features of the calculations of the two reactions. In Fig. 1, *b* we show the maxima of the velocity distributions for the different emitted isotopes as a function of the normalized impact parameter. It is seen that the velocity loss is very strongly correlated to the impact parameter. The dispersion of the points for different isotopes is small. This correlation is the same as the one seen in deep-inelastic reactions in so-called Wilczynski-plots [18] of the kinetic energy loss versus the scattering angle, which is strongly correlated to the impact parameter via the deflection function [9].

We see a clear difference in the two reactions. The dissipation in the two reactions is similar around and above the grazing distance. However, in the reaction on the Ta target the dissipation increases strongly with decreasing impact parameter and already leads to fusion for a value of the normalized impact parameter of about 0.7. On the other hand,

the dissipation is considerably weaker in the reaction on the Be target and binary reactions are seen for much smaller impact parameters. In other words, the O+Be reaction is considerably more transparent. We will see this feature also in other observables discussed below.

The isotope distributions are of primary interest with respect to the possibilities of producing new, and often neutron-rich, nuclei in heavy ion collisions. Isotope distributions are shown in the four panels of Fig. 2 as a function of the normalized impact parameter; in the right column for the Be target, in the left for the Ta target. The upper row (see Fig. 2, *a*, *b*) shows the results of the BNV calculations, i.e. the distribution of the primary projectile-like fragments, while the lower row (see Fig. 2, *c*, *d*) shows the result when including the de-excitation and evaporation as given by the statistical model code SMM. To present the information in a more compact way the sum of the isotope yields for each element is taken and the elements are indicated by the same symbol in all panels.

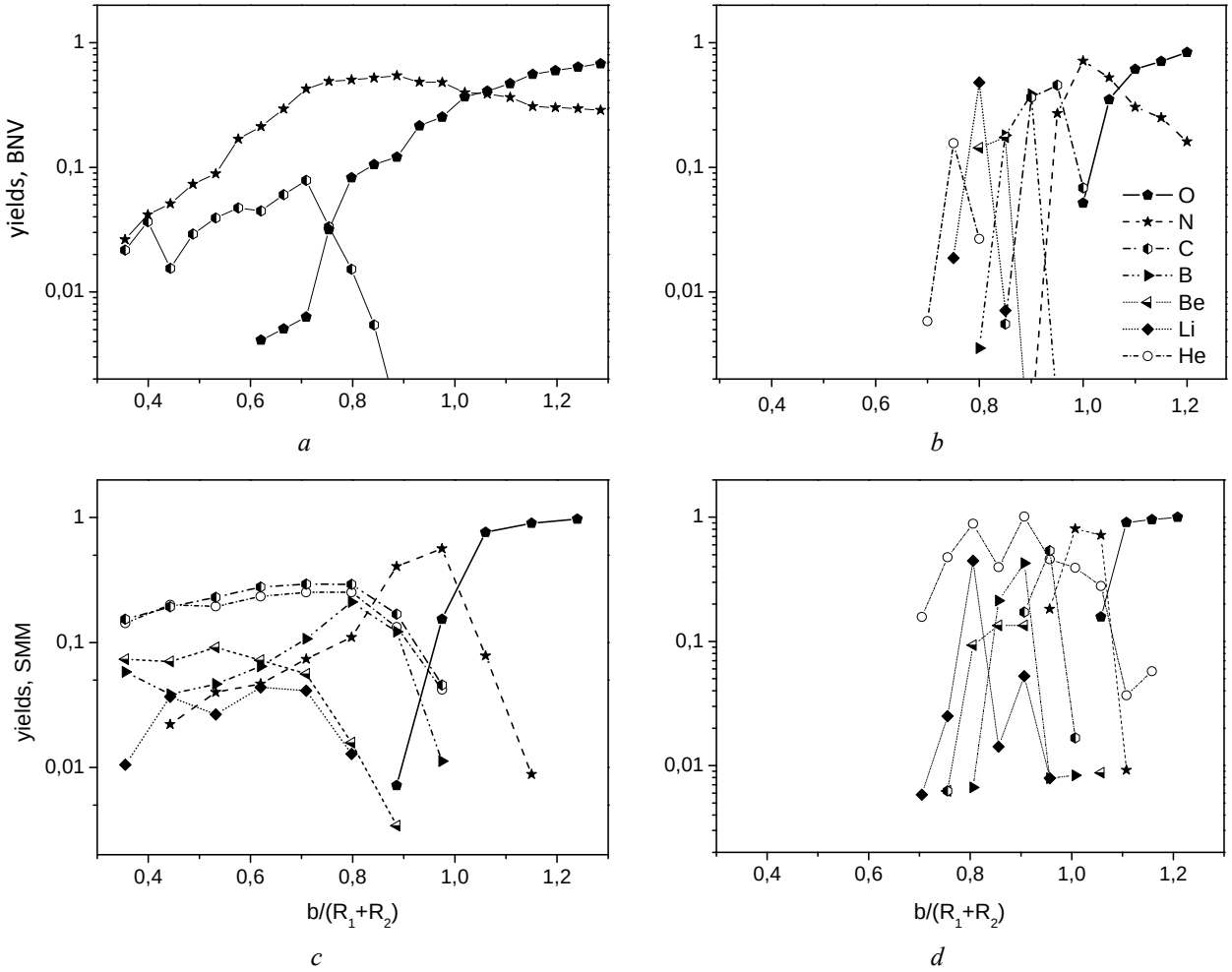

Fig. 2. Yields of different elements as a function of the normalized impact parameter for O + Be (*left*), and O + Ta (*right*): upper row: pure BNV calculations, i.e. primary fragments; lower row: after evaporation (SMM). Symbols distinguish different elements.

For the BNV calculations a larger transparency for the light Be target is seen again. The yield extends to much smaller impact parameters and produces only elements close to the projectile. For the Ta target isotopes with much larger mass loss from the projectile are emitted. After de-excitation (SMM, lower row of Fig. 2) the curves for the Ta target are not so different for the elements close to the projectile. This is understandable when considering that the evaporation proceeds predominantly by neutron emission, and that for the excitation energies in this case (shown in Fig. 1, *a*) on the average one neutron is emitted. Then this leads to similar element distributions before and after de-excitation. However, lighter elements, in particular He, appear also at larger impact parameters as decay products of the heavier isotopes. For the Be target the difference between BNV and SMM is considerably greater. By evaporation of protons lighter elements are generated and they appear as decay products for larger impact parameters.

The isotope distributions as a function of mass have been compared to experiment in [13]. Their

widths strongly depend on the opening angle for the forward detection. For the opening angle of the experiment the theoretical curves are too narrow, even with evaporation. However, small variations of the opening angle make the curves comparable to experiment.

In Fig. 3 we show calculated velocity spectra for projectile-like O and N fragments for the Be (see Fig. 3, *a*) and the Ta (Fig. 3, *b*) targets, given here for the full acceptance angle. The spectra are shown for the pure BNV calculations (round and triangular symbols) and after evaporation (SMM, square symbols). As mentioned above for these isotopes the de-excitation consists mainly of the evaporation of one neutron. Then the velocity distribution, e.g. for ^{15}N (SMM) should be similar to the one of ^{16}N (BNV) with some broadening. This is seen to be the case for the O + Ta reaction. For the Be target the velocity spectra are much broader already for the primary fragments (BNV). This is consistent with the much broader isotope distributions in Fig. 2, *a* and the velocity curves in Fig. 1, *b*. A comparison of the maxima of the velocity distributions for different isotopes with experiment is also given in [13], where we see that the shift of the velocity distributions by approximately one mass unit due to the evaporation of on the average one neutron leads to better agreement with experiment.

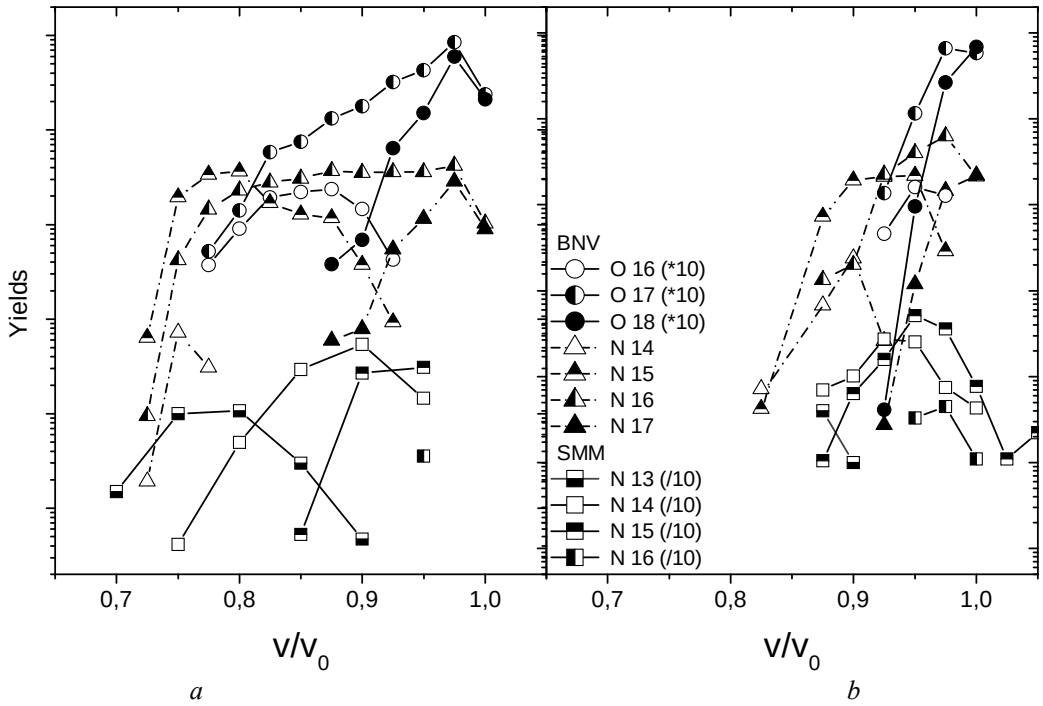

Fig. 3. Velocity distributions (ratio to beam velocity) of O and N isotopes in the reactions O + Be (*a*) and O + Ta (*b*). Shown are pure BNV calculations (O (round symbols, solid connecting lines) and N (triangular symbols, dash-dot lines)) and BNV + SMM calculations (N (square symbols, solid lines)).

Summary

We have investigated heavy ion collisions at Fermi energy in a transport description of the BNV type. The results are motivated by experimental data on very forward angle isotope yields and velocity distributions. In our approach we decompose the experimental yields empirically in terms of their velocity distributions into direct breakup (centered at beam velocity) and a dissipative deep-inelastic component (residual yield) [13]. We find that only the dissipative component is described by the transport approach, since the calculations give velocity distributions which always peak at velocities lower than the beam velocity. The direct component follows the systematics of the Goldhaber model with a width parameter that is in a reasonable range. A more microscopic description of the direct component would be desirable. The direct component is not reproduced by the transport calculations, because BNV includes only mean field dynamics (and dissipation in the collision term), but no direct nucleon-nucleon (NN) interactions. Probably a more direct reaction mechanism should account for this component [2].

We have investigated in detail the influence of the secondary evaporation of the primary excited fragments of the BNV calculation using a statistical model and an estimate of the excitation energies. This effect shifts and on the average broadens the isotope distributions. A detailed investigation of the impact parameter dependence helped to understand this behaviour. It improves the description of the

experimental data, even though they are still too narrow when restricting to the experimental angular range. We have further investigated the difference in the behavior of two collision systems with a light and a heavy target, respectively. We see that the mechanism of the two reactions is considerably different. For the lighter target a greater transparency and smaller dissipation is found, and binary reactions from a larger range of impact parameters are obtained.

It is hoped that with such studies a better understanding of the reaction mechanism and fragment production in Fermi energy domain is obtained.

This work has been supported by the Heisenberg - Landau program, by the Cluster of Excellence *Origin and Structure of the Universe* of the DFG, Germany, and in part by a Bogoliubov-Infeld grant of JINR (TM).

REFERENCES

1. *Souliotis G.A et al.,* Enhanced Production of Neutron-Rich Rare Isotopes in Peripheral Collisions at Fermi Energies // Phys. Rev. Lett. - 2003. - Vol. 91. - P. 022701-1.
2. *Tassan-Got L., Stephan C.* Deep inelastic transfers: A way to dissipate energy and angular momentum for reactions in the Fermi energy domain // Nucl. Phys. - 1991. - Vol. A524. - P. 121 - 140.
3. *Tarasov O.* Analysis of momentum distributions of projectile fragmentation products // Nucl. Phys. - 2004. - Vol. A734. - P. 536 - 540.
4. *Bacri Ch. O*. et al. Measurements in the beam direction of the 40Ar projectile fragmentation at 44 MeV/A // Nucl. Phys. - 1993. - Vol. A555. - P. 477 - 498.
5. *Borrel V. et al*. The decay modes of proton drip-line nuclei with A between 42 and 47 // Z. Phys. - 1992. - Vol. A344. - P. 135 - 144.
6. *Lahmer W. et al*. // Z. Phys. - 1990. - Vol. A337. - P. 425 - 437.
7. *Gelbke C.K. et al.* Transfer and fragmentation reactions of 14N at 60 MeV/u // Phys. Lett. - 1977. - Vol. B70. - P. 415 - 417
8. *Notani M. et al.* Projectile fragmentation reactions and production of nuclei near the neutron drip line // Phys. Rev.-2007. - Vol. C76. - P. 044605-1.
9. *Mikhailova T. et al.* Investigation of Dissipative Collisions with Transport Models // Romanian Jour. Physics. - 2008. - Vol. 52. - P. 875 - 893.
10. *Artukh A.G. et al.* Forward-Angle Yields of $2 \le Z \le 11$ Isotopes in the Reaction of ^{18}O (35 A MeV) with Be // Yad. Phys. - 2002. - Vol. 65. - P. 419 - 425.
11. *Artukh A.G. et al.* Forward-Angle Yields of $2 \le Z \le 11$ Isotopes in the Reaction of ^{22}Ne (40 A MeV) with Be // Proc. Int. Symp. on Exotic Nuclei (Lake Baikal, Russia, 2001) / Ed. by Yu.E. Penionzhkevich and E.A. Cherepanov. - Singapore: World Scientific P.C., 2002. - P. 269 - 276.
12. *Mikhailova T.I. et al.* Competition of Break-Up and dissipative processes in peripheral collisions at Fermi energies // Nucl. Physics and Atom. Energy. - 2009. - Vol. 10. - P. 45 - 49.
13. *Mikhailova T.I. et al.* Fragment production in peripheral heavy ion collisions at Fermi energies in transport models // Int. Journal of Modern Physics. - 2010. - Vol. E19. - P. 678 - 684.
14. *Goldhaber A.S.* Statistical models of fragmentation processes // Phys. Lett. - 1974. - Vol. B53. - P. 306 - 308.
15. *Bondorf J.P. et al.* Statistical multifragmentation of nuclei // Phys. Rep. - 1995. - Vol. 257. - P. 133 - 221.
16. *Bertsch G.F. Das Gupta S.* A guide to microscopic models for intermediate energy heavy ion collisions // Phys. Rep. - 1988. - Vol. 160. - P. 189 - 233.
17. *Baran V. et al.* Reaction dynamics with exotic nuclei // Phys. Rep. - 2005. - Vol. 410. - P. 335 - 466.
18. *Wilczynski J.* Nuclear molecules and nuclear friction // Phys. Lett. B. - 1973. - Vol. 47. - P. 484 - 486.

ДИСИПАТИВНІ ПРОЦЕСИ В $^{18}O + ^{9}Be$ І $^{18}O + ^{181}Ta$ РЕАКЦІЯХ ПРИ ЕНЕРГІЯХ ФЕРМІ

Б. Ердемчимег, Т. І. Михайлова, А. Г. Артюх, Г. Камінскі, Ю. М. Середа, М. Колонна, М. Ді Торо, Г. Г. Волтер

Наведено результати дослідження периферійних ядерних зіткнень при енергіях Фермі за допомогою транспортних моделей. Це мотивовано експериментами, що пов'язані з дослідженнями ізотопних виходів у реакціях ^{18}O на ^{9}Be та ^{181}Ta при E/A = 35 МеВ, виміряних під кутами, близькими до 0°. Дані мають двокомпонентну структуру: одна компонента при швидкості пучка (“пряма компонента”), а друга – з більш низькими швидкостями (“дисипативна компонента”). Показано, що розрахунки з використанням транспортних моделей описують основні особливості дисипативної компоненти реакції. У розрахунках брався до уваги статистичний розпад первинних збуджених продуктів фрагментації налітаючої частинки. Це покращує порівняння результатів розрахунків з експериментом. Установлено істотно різну поведінку дисипативної компоненти в реакціях з легкою та важкою мішенями.

Ключові слова: глибоконепружні реакції, транспортні моделі, енергія Фермі.

ДИССИПАТИВНЫЕ ПРОЦЕССЫ В $^{18}O + {}^{9}Be$ И $^{18}O + {}^{181}Ta$ РЕАКЦИЯХ ПРИ ЭНЕРГИЯХ ФЕРМИ

Б. Эрдемчимэг, Т. И. Михайлова, А. Г. Артюх, Г. Камински, Ю. М. Середа, М. Колонна, М. Ди Торо, Г. Г. Волтер

Приведены результаты исследования периферийных ядерных столкновений в области энергий Ферми с помощью транспортных моделей. Это мотивировано экспериментами, направленными на изучение выходов изотопов в реакциях ^{18}O на ^{9}Be и ^{181}Ta при E/A = 35 МэВ, измеренных под углами, близкими к 0°. Данные имеют двухкомпонентную структуру: одна расположена вблизи скорости налетающей частицы (“прямая компонента”), а вторая – при более низких скоростях (“диссипативная компонента”). Показано, что расчеты с использованием транспортных моделей описывают основные особенности диссипативной компоненты реакции. В расчетах принимался во внимание статистический распад первичных возбужденных продуктов фрагментации налетающей частицы. Это улучшает согласие результатов расчетов с экспериментом. Найдено значительное различие в поведении диссипативной компоненты в реакциях на легкой и тяжелой мишенях.

Ключевые слова: глубоконеупругие реакции, транспортные модели, энергия Ферми.

Received 07.06.10,
revised - 20.12.10.